

Common interatomic potential model for the lattice dynamics of several cuprates

S. L. Chaplot,* W. Reichardt, L. Pintschovius, and N. Pyka[†]

*Forschungszentrum Karlsruhe-Technik und Umwelt, Institut für Nukleare Festkörperphysik,
P.O.B. 3640, D-76021 Karlsruhe, Germany*

(Received 7 February 1995)

A common empirical model is developed for the lattice dynamics of the cuprates La_2CuO_4 , $(\text{La,Sr})_2\text{CuO}_4$, Nd_2CuO_4 , $\text{YBa}_2\text{Cu}_3\text{O}_6$, and $\text{YBa}_2\text{Cu}_3\text{O}_7$, which is also consistent with their crystal structures. Starting from the idea that the binding in these compounds is primarily ionic in character, the interatomic interactions were modeled using shell models with short-range repulsive potentials of the Born-Mayer type. For the metallic members of the series, screening of the ionic forces by free carriers was taken into account. There is clear evidence for an anisotropic Cu-O potential whereas the polarizabilities could be kept isotropic. The Cu(1)-O(4) bond in $\text{YBa}_2\text{Cu}_3\text{O}_6$ could not be treated on a common footing, as there is too little charge on the Cu(1). The present study demonstrates that the lattice dynamics of all the compounds investigated can be described quite satisfactorily by a common model and it offers a basis for extensions to related compounds. On the other hand, we found clear indications that a description of the lattice vibrations with purely ionic forces has its limits for this class of compounds.

I. INTRODUCTION

The general interest in the high- T_c superconductors stimulated numerous experimental as well as theoretical investigations of the lattice-dynamical properties of these materials. On the experimental side, inelastic neutron scattering has given very detailed information¹ about the phonons in the whole Brillouin zone (BZ). In addition, most of the zone-center phonons have been studied Raman and infrared experiments. On the theoretical side, there have been attempts to predict phonon frequencies by *ab initio* methods such as the frozen-phonon technique^{2,3} based on the local-density approximation (LDA). However, these attempts are presently limited to a few specific phonons at high-symmetry points of the BZ because of computational complexities. Therefore, empirical models were developed for the calculation of the complete phonon dispersion relation and of the phonon density of states (PDOS). First, such models are indispensable for the assignment of phonon peaks observed in inelastic neutron-scattering experiments.¹ Second, the models reveal some insight into the strength and the character of the interatomic forces. Third, one might hope that the models help to isolate anomalies in the phonon dispersion relations which are possibly due to a strong coupling of phonons to electrons.

Models used in early experimental investigations of the phonon dispersion curves¹ were primarily considered as interpolation schemes, i.e., the model parameters were fit to describe the experimental frequencies and intensities as closely as possible without imposing further constraints. At a later stage, attempts were made to reduce the number of parameters and to keep only those which lend themselves to an obvious physical interpretation. Very good agreement between model and experiment was achieved for several compounds,^{1,4} but some of the model parameters showed unexpectedly larger differences be-

tween the systems investigated. This could be tolerated in as far as the models were used as interpolation schemes only. However, when trying to exploit the models for elucidating the binding properties, we thought the situation to be unsatisfactory and felt the need for a common empirical model describing the lattice dynamics of all the cuprates investigated.

As it is widely accepted that the dominant interactions in the cuprates are of ionic type, a rigid-ion model or a shell model were the most obvious choices for the lattice dynamics. Based on previous attempts to describe the phonons in the cuprates¹ we opted for the shell model in spite of the larger number of parameters involved. For the metallic members of the family, an additional term was used representing the screening by free carriers. One of the aims of the present investigation was to explore to what extent this makes the shell model adequate also for the metallic compounds.

Whereas in shell models for individual compounds the short-range interactions may be described by force constants, force constants are impractical for a common model since they will vary between compounds because of different bond lengths. There have been attempts to obtain models based on interatomic potentials,⁵⁻⁷ which offer the possibility of using identical or nearly identical parameters for different system. However, these attempts severely suffered from the lack of a broad data base for the dynamical properties at their time. We are now in a much better situation in this respect and therefore decided to start afresh. We tried to find model parameters which are transferable among the different cuprates, are consistent with their crystal structures, and give a description of the phonons which is about equally good for all the systems investigated, i.e., La_2CuO_4 , $(\text{La,Sr})_2\text{CuO}_4$, Nd_2CuO_4 , $\text{YBa}_2\text{Cu}_3\text{O}_6$, and $\text{YBa}_2\text{Cu}_3\text{O}_7$. In such a scheme, the parameters of the interatomic potentials are open to physical interpretation and also allow

comparison between different atomic species. For instance, the short-ranged Born-Mayer potentials are indicative of the atomic radii. Details will be discussed later. Corrections to the shell model were considered only in those cases where serious shortcomings of the model description indicated a need to go beyond the framework of the shell model.

In respect to the ionic charges there is *a priori* an obvious problem for a common model: the requirement of charge neutrality cannot be fulfilled for all the compounds investigated with any universal choice of the ionic charges. This refers in particular to the compounds $\text{YBa}_2\text{Cu}_3\text{O}_6$ and $\text{YBa}_2\text{Cu}_3\text{O}_7$. We tried to keep the necessary adjustments of the ionic charges at a minimum.

The paper is organized as follows: in Sec. II we describe the interatomic potential in the shell model, in Sec. III we explain how the model parameters were determined, and in Sec. IV we present a comparison between model and experiment. Sections V and VI are devoted to a comparison with other lattice-dynamical models and to the conclusions, respectively.

II. INTERATOMIC POTENTIAL IN THE SHELL MODEL

In the shell model⁸ each atom k is represented by a core with charge $X(k)e$ and a shell with charge $Y(k)e$, which are coupled by a core-shell spring constant $K(k)$. The long-range interaction is given by the Coulomb interaction between these charges on the various atoms. The short-range interactions are assumed to act only between the shells, and are represented by the following interatomic potential:

$$V_{kk'}(r_{ij}) = A_{kk'} \exp(-r_{ij}/R_{kk'}) , \quad (1)$$

where r_{ij} is the distance between the two atoms i and j of species k and k' , respectively. $Z(k) = X(k) + Y(k)$, $Y(k)$, $K(k)$, $A_{kk'}$, and $R_{kk'}$ are the parameters of the potentials.

For the metallic compounds screening was taken into account by replacing the long-range Coulomb potential

$V_c(Q)$ by $V_c(Q)/\epsilon(Q)$. For the dielectric function $\epsilon(Q)$ we used the three-dimensional Lindhard function of the electron gas.⁹ The numerical evaluation of $V_c(Q)/\epsilon(Q)$ was based on the following expression:

$$\frac{V_c(Q)}{\epsilon(Q)} = V_c(Q) - \frac{\epsilon(Q) - 1}{\epsilon(Q)} V_c(Q) . \quad (2)$$

The first term on the right-hand side can be determined by Ewald's method. The second term can be treated entirely in Q space as $\epsilon(Q) - 1$ decreases like $1/Q^6$ for large Q .

In addition to the interactions discussed above, it may also be necessary to include van der Waals interactions. However, as van der Waals interactions are not the dominant ones in the cuprates, we saw no way to determine the strength of these interactions from the experimental data. Therefore, we included a van der Waals term

$$V_{kk'}(r_{ij}) = -C_{kk'}/r_{ij}^6 \quad (3)$$

only for oxygen-oxygen pairs, for which the value of $C_{kk'}$ was chosen in accordance with previous experience.^{6(b)} For all other pairs the van der Waals interaction was not explicitly taken into account.

The parameters of the models were refined by a least-squares fit to both the crystal structure and the available phonon frequencies in the various cuprates. We emphasize that it is essential to reproduce also the crystal structure, whereas this aspect is sometimes ignored in the literature with the argument that the potential is only used for the limited purpose of calculating force constants. First, a fit of the interatomic potential to the crystal structure makes use of a different kind of data than just phonon frequencies, thereby imposing serious constraints on the potential parameters. Second, a fit of the potential to the crystal structure ensures the rotational invariance of the force field. It is known¹⁰ that the second derivatives of the potential are related to the first derivatives via the rotational invariance conditions. For example, Eq. (23.23) in Born and Huang¹⁰ is

$$\delta_{\alpha\mu}\phi_\nu(k) - \delta_{\alpha\mu}\phi_\mu(k) = - \sum_{l'k'} \{ \Phi_{\alpha\nu}(0k, l'k') X_\nu(0k, l'k') - \Phi_{\alpha\nu}(0k, l'k') X_\mu(0k, l'k) \} , \quad (4)$$

where $X(l'k')$ is the position coordinate of the atom k' in the unit cell l' and $X(0k, l'k') = X(l'k') - X(0k)$, Φ_ν and $\Phi_{\alpha\nu}$ are the first and second derivatives of the potential energy, respectively, which correspond to the forces and the force constants. The lattice-dynamical formalism requires therefore that the right-hand side of Eq. (4) vanishes as one of the conditions of rotational invariance. This applies both to a potential model and to a force-constant model. For the former, the conditions are ensured if the potential produces a minimum at the crystal structure which is used for the calculation of the force constants. If, however, the potentials used are not com-

patible with the crystal structure, sound velocities in different directions, which should be equal by symmetry, may be very different from each other. An example of such a deficiency is found in Ref. 5(d), where two sound velocities given both by the elastic constant C_{55} were found to be $v = 1.8$ and 2.8×10^3 m/sec.

However, we did not attempt to impose the structural constraints rigorously but treated them in the same manner as the phonon frequencies. In other words, the model parameters were chosen as a compromise to give an optimum description of the phonon dispersion curves while keeping the forces and pressures at reasonably low

values. Hereby, the phonon frequencies were calculated for the experimental structure. We have adopted this procedure for convenience in computation and think that it is justified when fitting to data taken at elevated temperatures in structures involving some anharmonic interactions as in La_2CuO_4 .

III. TRANSFERABLE POTENTIALS

For determining the parameters of transferable potentials we first determined suitable parameters separately for tetragonal La_2CuO_4 and Nd_2CuO_4 , which have slightly different structures, known as the T and T' structures, respectively. This was done using an iterative least-squares fit to the available phonon frequencies¹ and to the crystal structure, i.e., minimizing the anisotropic external pressure to obtain the correct lattice constants and minimizing the forces on the atoms sitting at the equilibrium positions. The relative weights of the phonon data and the structure data were chosen so as to obtain a potential minimum very close to the observed structure. In this procedure, the phonon frequencies were always calculated for the observed structure (quasiharmonic approximation) rather than for the true potential minimum (harmonic approximation).

As the fit was based on 600-K data for La_2CuO_4 and 300-K data for Nd_2CuO_4 , the potential obtained was an effective one, i.e., including anharmonic effects. For Nd_2CuO_4 anharmonicity is not a serious problem, as this compound does not undergo a phase transition and only few phonons show a noticeable temperature dependence. On the other hand, there is significant anharmonicity in La_2CuO_4 associated with the tetragonal-to-orthorhombic phase transition. Therefore, it was not clear from the beginning how well an effective quasiharmonic potential might work for the T phase. It turned out that this approximation works in general quite well. As will be discussed later, there are only a few phonon branches which we suspect to be relatively poorly described because of the neglect of anharmonicity.

The separate models for La_2CuO_4 and Nd_2CuO_4 produced a mean deviation of 0.3 THz for about 500 observed and calculated frequencies in each case. When using independent force constant parameters for the various atomic pairs and anisotropic and different shell-model parameters for the two oxygen sites we obtained a further improvement of the fit quality to ~ 0.22 THz. This shows that the potential ansatz has some inherent limitations, but in view of large values of the frequencies involved (up to 20 THz) we regard a mean deviation of only 0.3 THz as very satisfactory.

We note that published models^{5-7,11} based on a limited database gave a much poorer agreement with experiment ($\Delta\nu=0.6$ THz or above). Even the model of Rampf *et al.*^{5(e)} for Nd_2CuO_4 which was fit to the neutron-scattering data does not agree with experiment as well as our potential model ($\Delta\nu=0.42$ THz).

Starting from the parameters of the separate models for La_2CuO_4 and Nd_2CuO_4 a common set of parameters for the two compounds was determined by iteration. In this procedure the $R_{KK'}$ parameters for the La-O and

Nd-O interactions, respectively, were deliberately treated as independent as they reflect the different ionic radii of the two three-valent ions.

The parameters of the Cu-O potential were not easily transferable from La_2CuO_4 to Nd_2CuO_4 . In La_2CuO_4 there was a clear need to use an anisotropic Cu-O potential with a significantly longer range along the c direction, in line with common wisdom that the oxygen octahedra are strongly elongated due to the Jahn-Teller effect. In the T' phase, however, the oxygen ions do not form octahedra, and consequently it is not evident whether the Cu-O(2) interaction in Nd_2CuO_4 can be treated like the Cu-O(2) interaction in La_2CuO_4 . The result of the fit to the Nd_2CuO_4 data was unexpected: the Cu-O(2) interaction was very long range which seems physically unreasonable. Therefore we did not make a compromise between the La_2CuO_4 and the Nd_2CuO_4 parameters for this type of potential, but used the La_2CuO_4 values for Nd_2CuO_4 as well. This entailed a significant loss in fit quality for Nd_2CuO_4 .

The model for $(\text{La,Sr})_2\text{CuO}_4$ was obtained from the model for insulating La_2CuO_4 by adding a term representing a screening of the Coulomb forces by free carriers. This procedure was justified by the fact the phonon dispersions of La_2CuO_4 and $\text{La}_{1.9}\text{Sr}_{0.1}\text{CuO}_4$ are very similar,¹ a major difference being the suppression of the LO-TO splittings at the zone center.

In a next step we tried to set up a model for $\text{YBa}_2\text{Cu}_3\text{O}_6(\text{O}_6)$ with parameters as close as possible to those of La_2CuO_4 and Nd_2CuO_4 . A principal problem for this transfer of parameters comes from the fact that the use of nominal charges will produce charge neutrality in La_2CuO_4 and Nd_2CuO_4 , but not in O_6 . This means that one or several of the positive ions in O_6 carry a smaller charge than is expected from the other compounds. Fits using the charges as free parameters strongly indicated that it is the Cu(1) which carries a very small charge. Ascribing a charge of only 0.4 to the Cu(1) allowed us to use the standard values of the charges for Cu(2,3) and O, the La/Nd charge for Y and a very reasonable value for the Ba charge, i.e., 84.5% of its nominal value. However, because of the small charge on Cu(1) the Cu(1)-O(4) bond could not be treated in the standard way, but was treated as a covalent one with special force constants describing its strength. On the other hand, the interaction between O and the in-plane Cu ions could be described by the parameters taken from $\text{La}_2\text{CuO}_4/\text{Nd}_2\text{CuO}_4$.

The transfer of parameters from O_6 to $\text{YBa}_2\text{Cu}_3\text{O}_7(\text{O}_7)$ is again complicated by the problem to maintain charge neutrality in spite of introducing an additional ion. Fits for O_7 with the charges as free parameters indicated that here the Cu(1) ion carries a relatively large charge. Hence we assigned the standard Cu charge also to Cu(1) and returned to the ionic picture for the Cu(1)-O(4) bond. Still this did not suffice to produce full charge neutrality. To this end we tried to adjust the ionic charges in several ways. The most satisfactory way was to reduce somewhat the charge on the chain O and to leave all other charges as in O_6 . As the bond distance

Cu(1)-O(4) is very close to the in-plane Cu(2)-O(2,3) distance, the same Born-Mayer parameters were used for both types of bonds. This means that the Cu(1)-O(4) bonds in O_7 were treated like the in-plane Cu-O bonds in La_2CuO_4 and the Cu(2)-O(4) bonds like the out-of-plane bonds in La_2CuO_4 . For the Cu(1)-O(1) interactions in O_7 it was natural to assume the same parameters as for Cu(2)-O(2,3). As in the case of $(La,Sr)_2CuO_4$ a term representing screening by free carriers was added to account for the metallic character of O_7 .

The parameters are listed in Table I. As can be seen from that table, our model involves ionic charges which are about 80% of the full ionic charges. This indicates that the interatomic interactions are largely ionic but not fully so. This is also consistent with previous models^{5-7,9} where it was general experience that models with similar fractional ionic charges produced a significantly improved description of the dynamics compared to those with full ionic charges. There is also a partial correlation in the shell model between the ionic charge and the polarizability, i.e., the effect of a large ionic charge on the frequencies is reduced by using a large polarizability. In the present model, however, the ionic charges also have to meet a strong constraint arising from the structure, and therefore the charges and the polarizability are to some extent determined independently.

A satisfactory description of the phonons required a consideration not only of the polarizability of the negative ions, but also of the positive ones. This result is surprising as it is intuitively thought that the rather small positive ions should have a very small polarizability. It is in particular the appreciable polarizability of the trivalent metal ions that we consider as unusual and specific to the cuprates. Extensions of these studies to simple perovskites of type ABO_3 like $SrTiO_3$, $LaAlO_3$, and $Ba_{1-x}K_xBiO_3$ showed that there is little improvement in the description of the phonons when allowance is made for the polarizability of the A ions. The need to ac-

TABLE I. Parameters of a unified shell model described in the text. $Z(k)$, ionic charge; $Y(k)$, shell charge; $K(k)$, core-shell force constant. $A_{kk'}$, $R_{kk'}$, parameters of the Born-Mayer potential; $C_{kk'}$, parameter of the van der Waals potential.

k	$Z(k)$	$Y(k)$	$K(k)$ (nm ⁻¹)
O[O(1) in O_7]	-1.56 (-1.26)	-3	1800
Cu	1.64	+3	2000
Cu(1) in O_6	0.40	0	∞
La,Nd,Y	2.30	-4	8000
Ba	1.69	+3	700
$k-k'$	$A_{kk'}$ (eV)	$R_{kk'}$ (Å)	$C_{kk'}$ (eV Å ⁶)
O-O	2000	0.284	100
Cu-O	3950	0.228	
Cu-O ⊥	460	0.353	
La-O	2000	0.324	
Nd-O	2000	0.316	
Y-O	2000	0.306	
Ba-O	2000	0.322	
Ba-Cu	2000	0.335	

count also for the polarizability of the positive ions indicates that a simple ionic picture is *not* fully adequate to describe the binding properties of the cuprates.

The sign of the shell charge was found to be negative for O, La, Nd, and Y, but positive for Cu and Ba. We cannot offer any explanation for this behavior. From extensive model calculations we learned that the dispersion curves are about equally well described when switching from a negative shell charge of the trivalent ion to a positive one and doubling its value while leaving all other model parameters unchanged. This procedure produces noticeable changes of the calculated frequencies, but as increased deviations between model and experiment at some places are compensated by improvements at other places the average deviation between model and experiment remains about the same. Therefore, our choice of a negative shell charge is somewhat arbitrary. We note that systematic studies based on more complex shell models than the transferable potential model did not yield a clear preference for a positive or a negative shell charge either. Only our finding that in some cases the phonon density of states is slightly better reproduced by models with negative shell charges tips the balance.

The $A_{kk'}$ parameters for O-O, La-O, Nd-O, Y-O, Ba-O, and Ba-Cu were found to be rather similar, i.e., differing by not more than a factor 1.4. We decided to use the same value $A_{kk'}=2000$ for most of them, so that the parameters $R_{kk'}$ can be expected to be proportional to the sum of the ionic radii. We tried to use $A_{kk'}=2000$ for the Cu-O interactions as well and obtained $R_{kk'}=0.25$ Å and, 0.29 Å for the in-plane and out-of-plane interactions, respectively. With this choice the anisotropy of the Cu wave function discussed above is reflected in the $R_{kk'}$ parameters only. However, using also different $A_{kk'}$ values for the in-plane and the out-of-plane Cu-O interactions led to a significant improvement in the description of the structure and the phonon frequencies.

It is gratifying that the resulting $R_{kk'}$ parameters of the La-O, Nd-O, and Y-O interactions scale well with the sum of the corresponding ionic radii. Thus, very similar results would have been obtained if we would have imposed such a scaling as a restriction in the calculations from the very beginning. The close correlation between the range of the repulsive potential determined from lattice-dynamical models and effective ionic radii was already noted earlier [e.g., in Ref. 6(a)]. From this experience we conclude that when the model is to be applied to other members of the cuprate family containing over trivalent ions the $R_{kk'}$ parameters might be obtained via tabulated values of the ionic radii.

All the above short-ranged interactions involve primarily the first-neighbor atomic pairs, although we did not cut off the potentials beyond the first neighbors. In general, we tried to consider only the short-range interactions between cations and anions, but in the 123 compounds we found it necessary to include a metal-metal interaction (Cu-Ba). Although the corresponding longitudinal force constants are only a few percent of the largest force constants in these systems, they appear to be important for the shear stability of the lattice.

TABLE II. Pressures p_i and forces f_i on the atoms when imposing the structural parameters listed in Table I. The forces refer to the atoms in the lower half of the elementary cell. F and G are longitudinal and transverse force constants, respectively.

Compound	$\langle \Delta\nu \rangle$ (THz)	Special f.c (nm ⁻¹)	$\langle p \rangle$ (GPa)	p_x, p_y (GPa)	p_z (GPa)	$f(\text{La, Nd, Ba})$ (eV/Å)	$f(\text{Cu}_2)$ (eV/Å)	$f(\text{O}_2, \text{O}_3)$ (eV/Å)	$f(\text{O}_4)$ (eV/Å)
La ₂ CuO ₄	0.332		0.52	-0.77	3.09	0.28			-0.44
La ₂ CuO ₄	0.325	$G[\text{La-O}(2)]=2.0$	-0.27	-0.77	0.73	-0.01			-0.14
Nd ₂ CuO ₄	0.501		0.48	1.28	-1.12	-0.09			
Nd ₂ CuO ₄	0.325	$F[\text{Cu-O}(2)]=8.5$	0.48	1.28	-1.12	-0.09			
YBa ₂ Cu ₃ O ₆	0.316	$F[\text{Cu}(1)\text{-O}(4)]=321$ $G[\text{Cu}(1)\text{-O}(4)]=-5.7$	-0.69	-1.63	1.19	-0.77	-1.08	1.05	-0.34
YBa ₂ Cu ₃ O ₇	0.362	$G[\text{O}(1)\text{-O}(4)]=5.0$	-0.14	-0.73	1.08	1.93	0.18	0.29	-2.53
YBa ₂ Cu ₃ O ₇	0.388	$F[\text{Ba-O}(1)]=25$	2.09	-0.73	4.26	1.93	0.18	0.29	-1.61
				2.73				0.21	

IV. COMPARISON WITH EXPERIMENT

In this section the model calculations using the potential parameters of Tables I and II are compared to the phonon data obtained by inelastic neutron scattering. Force constants arising from a special treatment of an interaction are given in Table II. The same table also lists the internal pressures and the forces acting on the ions at nonsymmetry positions for the various models. The structural parameters used in the calculations are listed in Table III.

A. (La, Sr)₂CuO₄

Figure 1 shows a comparison of the calculated and experimental¹ phonon dispersion curves of La₂CuO₄. The mean deviation is only $\langle \Delta\nu \rangle = 0.33$ THz which we consider as small and close to the limits of a simple pair-potential model in the quasiharmonic approximation. The good agreement between theory and experiment is corroborated by a comparison of the calculated and the experimental¹² phonon density of states (see Fig. 2).

In the calculation that led to the dispersion curves displayed in Fig. 1, a small transverse force constant of $G[\text{La-O}(2)] = 2.0$ (Nm⁻¹) has been included into the model. Without this additional parameter the tilt mode associated with the lowest Δ_4 frequency at (0.5, 0.5, 0) is slightly unstable [$\nu^2 = -0.25$ (THz²)]. This result appears to be reasonable as at low temperatures La₂CuO₄ is orthorhombic and the high-temperature tetragonal phase is stabilized only by anharmonic forces. The additional parameter has little influence on the rest of the phonon branches, but also produces an improved reproduction of the structural constraints.

Fil *et al.*¹³ argued that the quadrupolar mode which is the highest Σ_3 mode at X [$q = (0.5, 0.5, 0)$] should be very low in frequency due to an interaction of the copper d orbitals with the lattice (we note that the theory was carried out for insulating La₂CuO₄). We find that most of the frequency drop in the highest Σ_3 branch between Γ and X is accounted for by our potential model, and hence only the residual deviation of $\Delta\nu = 1.3$ THz at X may be attributed to the effect investigated by Fil *et al.*¹³ The dot-

dashed lines in Fig. 1 show the changes in the topmost Δ_1 and Σ_3 branches resulting from an additional quadrupolar term in the dynamical matrix. The quadrupolar force constant is about one-fourth of the value given in Ref. 13.

The frequency of the breathing mode which is the highest Σ_1 mode at X comes out in very good agreement with experiment. This confirms the view that the breathing mode is not anomalously soft, in contrast to a theoretical prediction by Weber,¹⁴ but in agreement with results of frozen-phonon calculations reported by Cohen, Pickett, and Krakauer.²

Figure 3 shows calculated and experimental phonon dispersion curves of La_{1.9}Sr_{0.1}CuO₄. The calculated curves are based on the model for undoped La₂CuO₄ after incorporation of a term representing screening by free carriers. Changes of the lattice parameters and of the effective mass of the ions on the La site upon doping have been ignored. The small mass defect affects only a few low-frequency branches with a maximum frequency shift of less than 1%.

Our first attempts to consider screening by using the simple Lindhard function⁹ as described in Sec. II were not fully satisfactory. We found that the data are better reproduced when the Lindhard dielectric function is modified to include exchange and correlation according to Geldart and Vosko.¹⁵ This type of dielectric function

TABLE III. Structural parameters of the compounds investigated.

	La ₂ CuO ₄	Nd ₂ CuO ₄	YBa ₂ Cu ₃ O ₆	YBa ₂ Cu ₃ O ₇
a (Å)	3.7817	3.945	3.840	3.8178
b (Å)				3.8835
c (Å)	13.2487	12.17	11.77	11.6828
z (La, Nd, Ba)	0.3608	0.3513	0.1948	0.1844
z [Cu(2)]			0.3609	0.3552
z [O(2)]			0.3793	0.3779
z [O(3)]				0.3779
z (O-apex)	0.1824		0.1521	0.1588

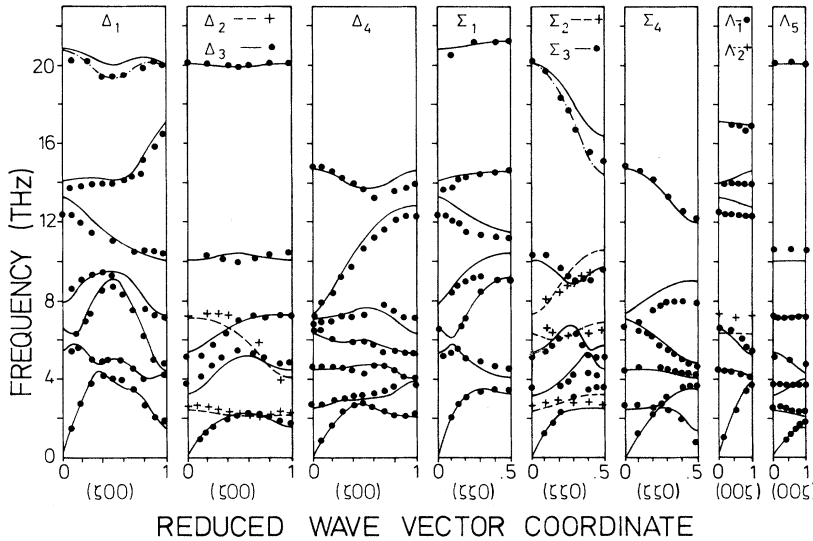


FIG. 1. Calculated (solid and dashed lines) and experimental (Ref. 1) phonon dispersion curves of La_2CuO_4 . The dash-dotted lines are obtained after including a special quadrupolar force constant.

gave a good description of the screening in SrTiO_3 doped with Nb.¹⁶ The Fermi wave number was calculated from the nominal number of free carriers to be $k_f = 0.315 \text{ \AA}^{-1}$. Using the relation $k_s^2 = 2.406 \times 10^8 m^* k_f / \epsilon_\infty$ together with $m^* = 1$, $\epsilon_\infty = 5$ a screening wave number $k_s = 0.39 \text{ \AA}^{-1}$ was obtained. Attempts were made to see if anisotropy of the screening is needed: it turned out that anisotropic screening does not lead to substantial improvements of the fit quality, and therefore we report here results on isotropic screening only.

It is evident from Fig. 3 that most of the observed differences between the phonon dispersion curves of doped and undoped La_2CuO_4 can be explained by screening by free carriers (Fig. 3 shows only those representations where our simple screening mechanism has produced observable changes in the dispersion curves). However, the strong frequency decrease upon doping in the highest Δ_1 branch around $q = (0.5, 0, 0)$ cannot be accounted for by free-carrier screening, and hence the agreement between model and experiment is poor for these specific phonons ($\Delta\nu \approx 2.5 \text{ THz}$). We presume that

a good description also of these phonons is beyond the capability of a simple model, i.e., that the behavior of the highest Δ_1 branch has to be considered as a phonon anomaly like those observed in conventional superconductors.

B. Nd_2CuO_4 (T' structure compounds)

The comparison of calculated and experimental phonon dispersion curves is shown in Fig. 4. The agreement between model and experiment is not quite as good as in La_2CuO_4 (the mean deviation is $\Delta\nu = 0.50 \text{ THz}$), but still satisfactory, as there is no serious discrepancy for any of the phonon branches investigated. By changing a single longitudinal force constant, i.e., that of the Cu-O(2) interaction, it is possible to achieve the same fit quality as for La_2CuO_4 (see Fig. 5). The extra force constant is only

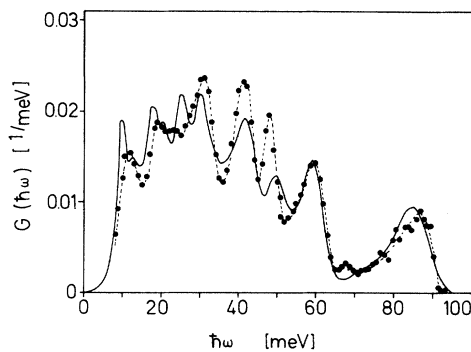


FIG. 2. Comparison of the calculated neutron-cross-section-weighted phonon density of states of La_2CuO_4 with the experimental data of Ref. 12.

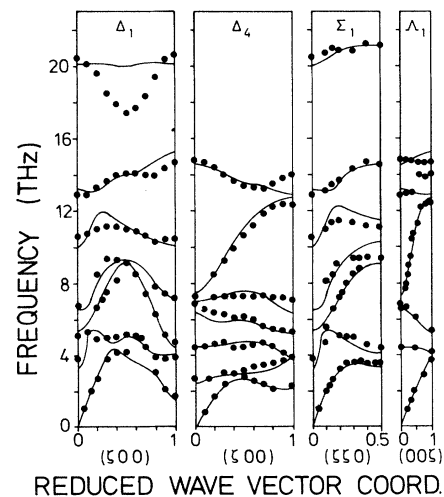


FIG. 3. Calculated (solid lines) and experimental (Ref. 1) phonon curves of $\text{La}_{1.9}\text{Sr}_{0.1}\text{CuO}_4$.

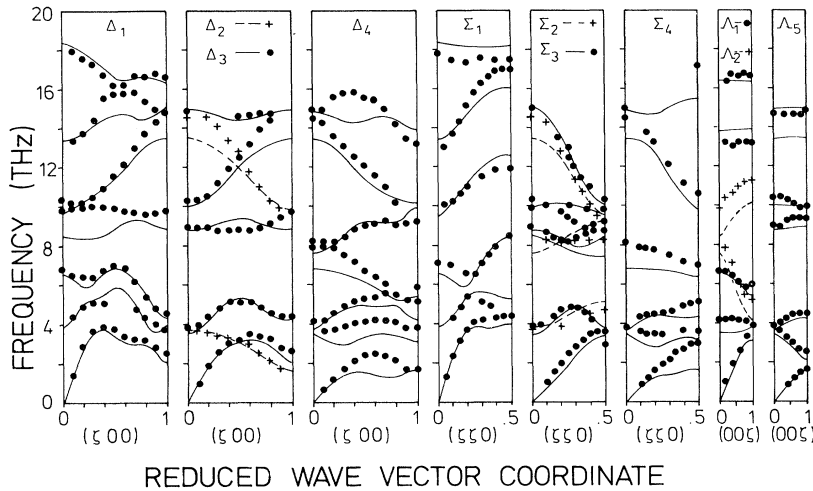


FIG. 4. Calculated (solid lines) and experimental (Ref. 1) phonon dispersion curves of Nd_2CuO_4 .

about 5% of the largest force constant in the system, but is nevertheless important for an accurate description of the phonon frequencies. In particular the low-frequency branches of Δ_4 and Σ_4 symmetry are then much better described.

As the Cu-Nd distance is smaller than the Cu-O(2) distance one may think that inclusion of the Cu-Nd interaction is a more plausible way to improve the model than stiffening the Cu-O(2) interaction. We checked this possibility and found that inclusion of the Nd-Cu interaction is indeed helpful, but that tuning the Cu-O(2) interaction leads to better results.

It has been shown by Pyka *et al.*¹⁷ that Nd_2CuO_4 is close to an instability where the four O(1) atoms surrounding a copper atom rotate as a rigid entity around an (001) axis. The corresponding soft mode is an X-point phonon of Σ_3 symmetry. The frequency of the soft rotational mode comes out somewhat too high in the calculations for both sets of model parameters discussed above,

i.e., at $\nu=3.8$ and 4.2 THz, respectively, whereas the experimental value is $\nu\approx 3.2$ THz at $T=300$ K and $\nu=2.9$ THz at $T=5$ K. However, the rotational frequency is very sensitive to the Nd radius. The model is able to correctly reproduce the fact that the rotational mode becomes unstable in Gd_2CuO_4 .¹⁸ Gd is a slightly smaller ion than Nd which can be accounted for by reducing the $R_{\text{Nd-O}}$ parameter by 3%. This produces the observed reduction in the lattice parameters as well as an unstable rotational mode, while practically all other phonon frequencies are very little affected.

Structural changes in going from Nd_2CuO_4 to Pr_2CuO_4 are only about 30% of those in going from Gd_2CuO_4 to Nd_2CuO_4 . Nevertheless, the B_u - and the B_g -mode frequencies differ considerably ($\Delta\nu/\nu\approx 10\%$) between Nd_2CuO_4 and Pr_2CuO_4 .^{19,20} [These modes involve out-of-plane elongations of O(1) or O(2) ions, respectively.] Our potential model is unable to reproduce these unexpectedly large differences.

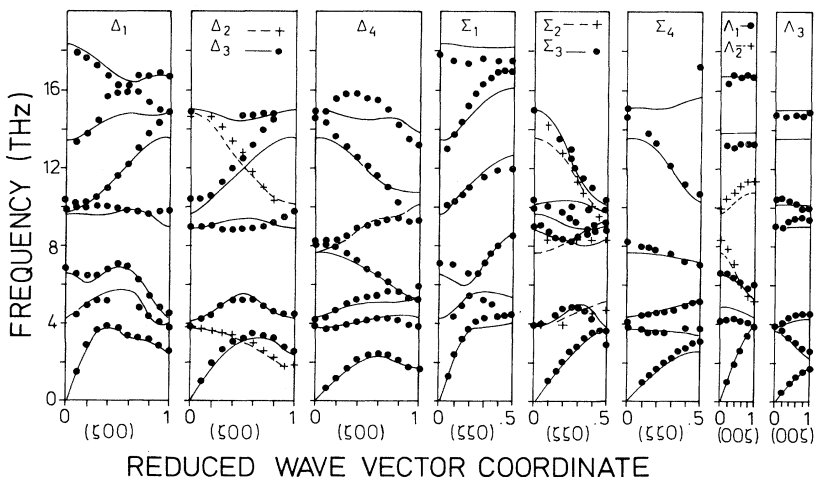


FIG. 5. The same as in Fig. 4, but using an extension of the transferable potential by tuning the longitudinal force constant of the Cu-O(2) interaction.

C. $\text{YBa}_2\text{Cu}_3\text{O}_6$

The comparison of the calculated results and the available experimental dispersion relation is presented in Fig. 6. The calculated neutron-cross-section-weighted phonon density of states is compared with the experimental²¹ density of states in Fig. 7. As noted earlier, the model results are satisfactory. However, the description of the structure is not fully satisfactory (see Table III). Fine-tuning of the parameters led to limited improvement only. We found that substantial improvements require a general reduction of the ionic charges.

Earlier^{1,4} it was found difficult to describe the splitting of the two-planar-oxygen scissor modes at $(0.5, 0.5, 0)$ corresponding to the in-phase and the out-of-phase motions in the Cu-O planes. We find that the effect is as-

sociated with an appreciable polarizability of the yttrium atom. This applies both to O_6 and O_7 . On the other hand, we found no means to reproduce the relatively large splitting of the in-phase and out-of-phase ab -plane polarized apical oxygen modes observed in experiment ($\Delta\nu=1.8$ THz) as compared to the calculated value $\Delta\nu=0.5$ THz (see in Fig. 6 the λ_5 branches at 6.6 and 6.1 THz, respectively and the corresponding data points at 7.5 and 5.7 THz, respectively). A three-body $\text{O}(4)\text{-Cu}(1)\text{-O}(4)$ bond angle stiffening force would reduce the discrepancy, but is beyond the framework of our model.

There is still a controversy concerning the highest A_g frequency associated with symmetric bond stretching vibrations of the apical oxygen. From Raman experiments on ceramic O_6 samples a value of ~ 14.2 THz was deduced²² whereas Burns *et al.*²³ determined a frequency of

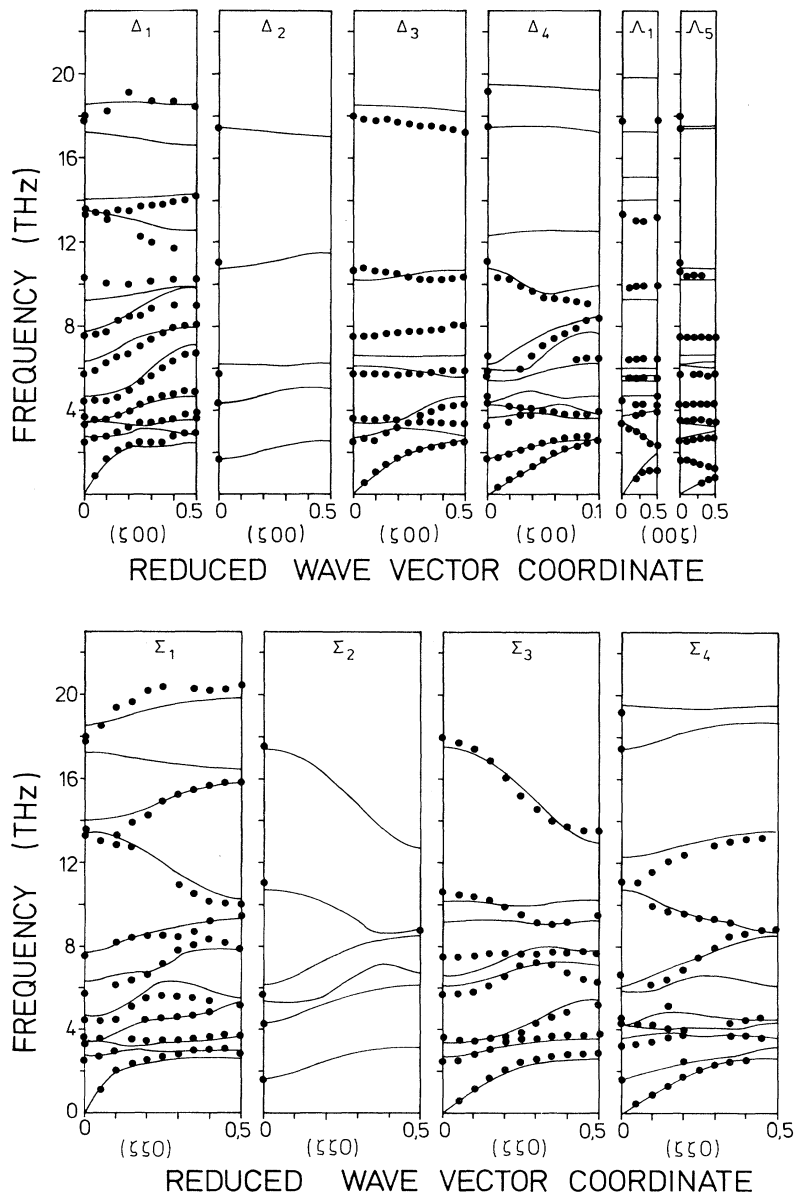


FIG. 6. Calculated (solid lines) and experimental (Ref. 1) phonon dispersion curves of O_6 .

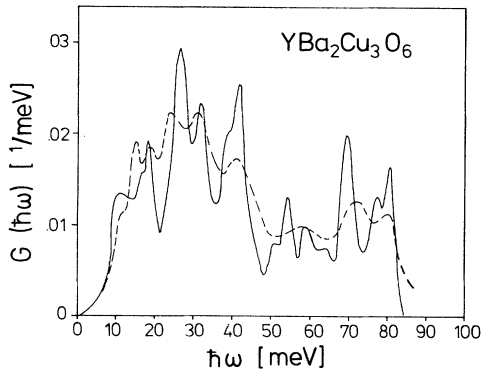


FIG. 7. Comparison of the calculated neutron-cross-section-weighted phonon density of states of O_6 (solid line) with the experimental data of Ref. 21.

18 THz from a single-crystal sample. Our model predicts a value of 17.2 THz which is closer to Burns' results.

D. $YBa_2Cu_3O_7$

Both the structure and the phonons are not as well described for O_7 as for the other compounds investigated. Serious discrepancies are found for the modes associated with the transverse chain oxygen vibrations. In particular, the calculated ab -plane polarized modes are too low in frequency and are even unstable at Γ , whereas the frequencies of the c -axis polarized modes are somewhat overestimated: The frequencies of the two A_u modes which involve a strong elongation of the chain oxygen are predicted at 10.8 and 9.4 THz, respectively, whereas the experimental values are 9.0 and 8.25 THz, respectively.

An unstable chain oxygen mode was predicted by Cohen, Pickett, and Krakauer on the basis of frozen-phonon calculations.² This calculation was done at the zone boundary of the $[0\xi 0]$ direction, where the elongation is of zigzag type and there is little interaction with other modes. In our model, however, this mode is stable and its frequency is rather high, in agreement with experiment.²⁴ At Γ , where our model predicts an instability, there is a strong mixing with other modes, in particular with those involving elongations of the apical oxygen. A detailed analysis showed that the chain oxygen ions sit in a nearly harmonic single-well potential if there is no coupling to the displacements of the other atoms. However, coupling to the displacements of the apical oxygen leads to a double-well potential with the minima separated by 1 Å. We checked experimentally whether the chain oxygen vibrations might be stabilized by anharmonic effects. However, in experiment the phonon mode in question shows a close to harmonic behavior with no significant temperature dependence of the frequency and the linewidth.

We made several attempts to avoid the instability and to raise the calculated frequency to the experimental value. It turned out that, while we retain the other parameters, we need a large transverse force constant of 5

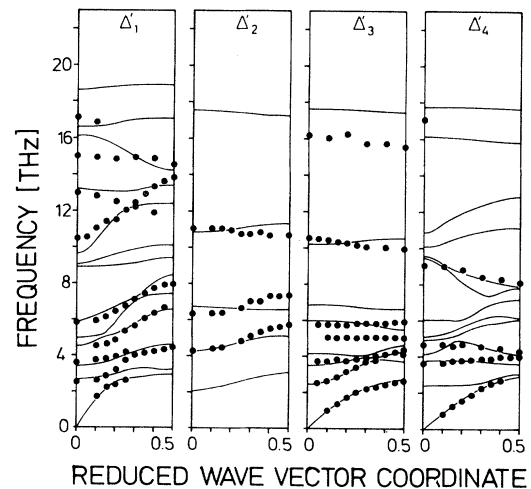
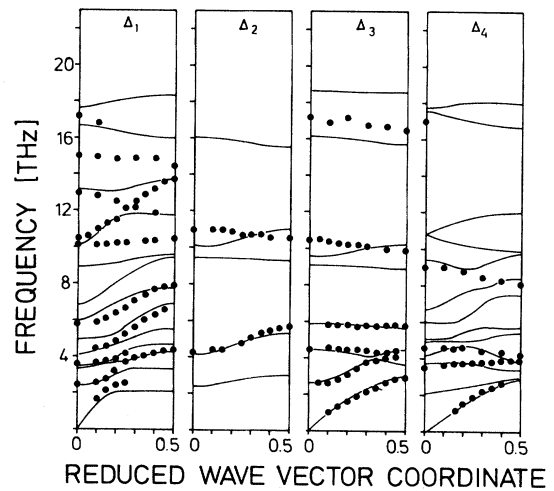
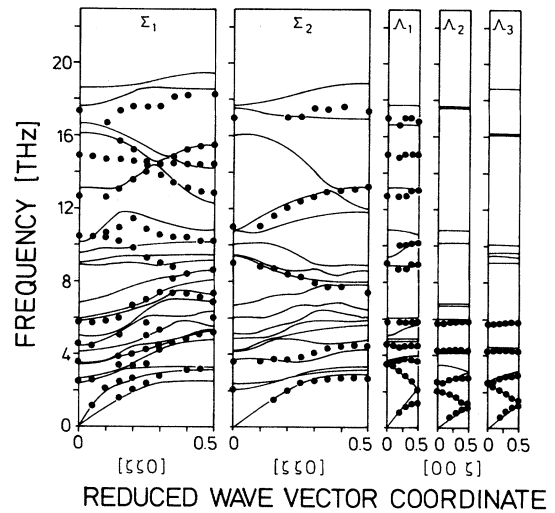


FIG. 8. Calculated (solid lines) and experimental (Ref. 1) phonon dispersion curves of O_7 . The primed labels refer to the $[0\xi 0]$ direction.

Nm^{-1} between O(4) and O(1) or an increase by $\sim 50\%$ in the longitudinal Ba-O(1) force constant of 25 Nm^{-1} . Both the proposals are not justified otherwise and perhaps they mimic features which are omitted in the model. They do not influence appreciably the rest of the dispersion curves and lead to about the same quality in the description of the data. The dispersion curves displayed in Fig. 8 were calculated with the parameters of Table I plus an additional transverse O(4)-O(1) force constant of 5 Nm^{-1} . Screening was done in the same manner as for doped La_2CuO_4 assuming 0.5 free carriers per formula unit ($k_f = 0.441 \text{ \AA}^{-1}$, $k_s = 0.461 \text{ \AA}^{-1}$).

The large splitting between the frequencies of the transverse *ab*-plane and *c*-axis polarized chain oxygen modes predicted by the model is essentially given by the Coulomb interaction between O(1) and O(4). Therefore a reduction of the charges on O(1) and O(4) would simultaneously reduce the discrepancies for both types of modes which is another indication that O_7 is less ionic than treated in our transferable model.

The phonon density of states O_7 is not as well reproduced by the model as for O_6 (see Fig. 9). This confirms former conclusions¹ that the differences in the phonon densities of states of O_6 and O_7 cannot be explained solely by structural changes. In particular, the pronounced high-frequency peak at 77 meV predicted by the model is shifted to lower energies in experiment. This is associated with the anomalous phonon softening observed for the in-plane Cu-O bond-stretching vibrations of O_7 discussed in Ref. 25. Another major discrepancy is the position of the pronounced peak in the middle of the spectrum which is predicted too low by about 5 meV. The strongest contribution to this peak stems from vibrations of the oxygen ions in the planes.

The mean-squared thermal amplitudes at 300 K calculated from our model are in good agreement with experiment²⁶ (Table IV), except for certain components: U_{33} of O(1) comes out too low, since the corresponding frequencies are calculated too high; U_{11} of O(1) is found in excellent agreement with experiment, since the *ab*-plane polarized transverse O(1) vibrations were stabilized by an *ad hoc* transverse O(1)-O(4) force constant. The large pre-

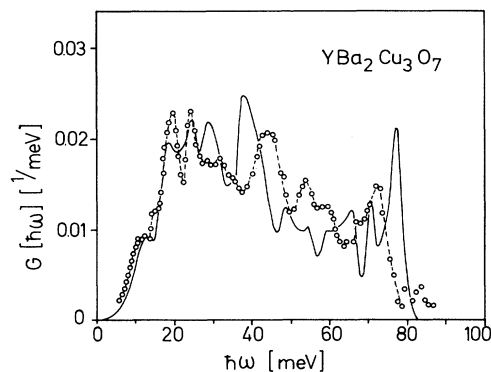


FIG. 9. Comparison of the calculated neutron-cross-section-weighted phonon density of states (solid line) with the experimental data of Ref. 21.

TABLE IV. Mean-squared thermal amplitudes in $\text{YBa}_2\text{Cu}_3\text{O}_7$ at 300 K in 10^{-4} \AA^2 . [The experimental analysis (Ref. 24) assumes $U_{11}=U_{22}$ except for the chain oxygen atom.] Errors in the calculated values due to the limited number of sampling points (14 415 points in the irreducible part of the BZ) are smaller than $1 \times 10^{-4} \text{ \AA}^2$.

Atom	Experiment (Ref. 22)			Model		
	U_{11}	U_{22}	U_{33}	U_{11}	U_{22}	U_{33}
Y	52		50	39	40	56
Ba	68		68	61	62	67
Cu(1)	66		50	99	39	46
Cu(2)	37		70	37	38	64
O(2,3)	69		87	51	53	107
O(4)	105		65	112	72	54
O(1)	222	72	130	221	43	79

dicted *ab*-anisotropy of the Cu(1) displacements was not addressed in the evaluation of the diffraction data.

The 9 elastic constants of O_7 were determined from 21 slopes of the acoustic branches in 7 different directions by a least-squares fit. They are listed in Table V. The agreement with the experimental values of Lei *et al.*²⁷ is very satisfactory. As can be seen from Table VI the consistency between the velocities of sound calculated directly from the model and those calculated from the elastic constants given in the first line of Table V is excellent in nearly all cases. The largest discrepancy occurs for the sound velocities determined by C_{55} , where the model yields $v=2.62$ (km/sec) for the 100 direction and $v=2.81$ (km/sec) for the 001 direction. The elastic constants yield $v=2.71$ (km/sec) for both cases. These slight inconsistencies are the consequence of the fact that the structural constraints were not rigorously fulfilled.

V. COMPARISON WITH OTHER LATTICE-DYNAMICAL MODELS

As was mentioned in the Introduction, a variety of models have been proposed in the literature for the lattice dynamics of the cuprates, and one may ask how these models compare with that presented in this paper. There is a basic similarity between all these models in that they start from an ionic picture of the binding properties with charges close to or even equal to the valency of the ions. However, there is a wide fluctuation of the other model parameters for several reasons.

(i) The models have a different degree of complexity, and when a model is refined by including further degrees of freedom this has effects on the other parameters. For

TABLE V. Elastic constants in GPa of $\text{YBa}_2\text{Cu}_3\text{O}_7$. The values extracted from the model are compared to results from ultrasound measurements (Ref. 25).

Source	C_{11}	C_{22}	C_{33}	C_{44}	C_{55}	C_{66}	C_{12}	C_{13}	C_{23}
Present work	221	260	186	64	47	102	116	76	80
Ref. 24	231	268	186	49	37	95	132	71	95

TABLE VI. Velocities of sound in km/s of $\text{YBa}_2\text{Cu}_3\text{O}_7$ in various directions of the reciprocal lattice as calculated from the model and the 9 elastic constants given in the first line of Table V.

Direction	Model			El. constant		
100	5.88	4.00	2.62	5.88	4.00	2.71
010	6.38	4.00	3.21	6.38	4.00	3.17
001	5.40	3.14	2.81	5.40	3.17	2.71
110	6.62	3.12	2.93	6.63	3.11	2.95
103	5.42	3.60	3.15	5.42	3.61	3.14
013	5.85	3.46	3.30	5.84	3.42	3.28
113	6.07	3.30	3.06	6.07	3.31	3.05

instance, going from the rigid-ion model to the shell model will lead to larger ionic charges and as a consequence to larger repulsive short-range forces. When corrections to the basic ionic models are considered, such as a partially covalent interatomic potential,^{6(b)–6(e)} a bond-angle potential²⁸ or quadrupolar interactions²⁹ there is likewise a strong effect on the other parameters.

(ii) Most of the models were developed for individual compounds. The parameters correspond to an optimum of the fit quality for the compound under investigation. Experience has shown that there are practically always other combinations of parameters which give nearly as good a fit quality. For these local optima some of the parameters may be very different from those of the true optimum. Transferability is a criterion which will favor one of these suboptimal parameter sets over the optimal one.

(iii) Not all the models were developed using structure constraints. We found structure constraints to be useful in many ways: they help (i) to restrict the least-squares-fit parameters into a physically meaningful domain (like transferability of the potential), (ii) to ensure that the direction dependence of the sound velocities is consistent with the symmetry of the crystal structure, and (iii) to differentiate between anisotropic interactions and anisotropic polarizabilities. The present model emphasizes anisotropic Cu-O interactions for both the structure and the dynamics and suggests that the anisotropy of the polarizability of the oxygen atoms may not be as large as previously supposed.

Among the various groups who presented lattice-dynamical models for the cuprates only two of them [Ref. 5(a)–5(e) and Chaplot and coworkers⁶] aimed at transferable potentials.

The authors of Ref. 5(a)–5(e) took the starting values of potential parameters from simpler structures for which reliable information was available. Subsequently, the parameters were refined on the basis of certain requirements such as obtaining a stable lattice and reproducing phonon frequencies observed by Raman scattering. It turned out, however, that the final parameter values reported for La_2CuO_4 [Ref. 5(a)] and $\text{YBa}_2\text{Cu}_3\text{O}_7$ [Ref. 5(b)] are very different. Recently, when the same ansatz was used for Nd_2CuO_4 ,^{5(c)} the resulting potential parameters were again very different from the previous two cases. These large differences can be understood from the fact that in the end each model was tuned to reproduce the data of a

single compound, and therefore not enough restraints were imposed on the parameters to arrive at a really transferable potential (see the discussion above). The strong modifications of the parameters resulting from tuning the model to specific data are illustrated by comparing the two models presented for Nd_2CuO_4 by this group (Rampf *et al.*^{5(e)}). The two models aimed at a description of both the structure and the dynamics. The second model was a refined version of the first one using published phonon data.¹ It is important to note that the refinement led to a strong reduction of the supposed anisotropy of the oxygen polarizability, and even reversed the anisotropy for one of the two oxygen sites (which were treated differently in their model). This confirms our view that anisotropic polarizabilities of the oxygen atoms are not essential in the cuprates.

In Ref. 6, rigid-ion potential models were reported for O_7 which were based essentially on the structure, as very little dynamical data were available. Construction of the models was guided by experience with other perovskites. In contrast to the present model all metal-metal interactions were included and the planar Cu-O interactions were treated in a special way to account for covalency of the bonds. The model of Ref. 6(c) produced a good description of the low-frequency phonons involving the vibrations of the cations and the elastic constants came out close to experiment. The high-frequency phonons were not as well reproduced as the low-frequency ones and therefore the mean deviation between calculation and experiment was considerably larger than for our present model ($\Delta\nu=0.9$ THz). This is not unexpected in view of the simplicity of the model (an unscreened rigid-ion model) and the small database used. We found that a substantial improvement of this model can be achieved by using the same screening formalism as applied in this work ($\Delta\nu=0.67$ THz).

The potential determined for O_7 [Refs. 6(a)–6(c)] was found to be transferable to Tl and La compounds^{6(d),6(e)} for the description of their structures and dynamics. [An earlier paper^{6(f)} had reported an independent model for the La systems with parameters similar but not identical to those given for O_7 in Refs. 6(a)–6(c).] The description was of about the same quality as in the case of O_7 , i.e., satisfactory but quantitatively not matching the description achieved by the models presented in this paper.

We would like to emphasize that the rigid-ion model for O_7 gave a good description of the dynamical behavior at high temperatures.^{6(b)–6(d)} The present model has yet to be tested in this respect, but we do not expect that this test will reveal serious shortcomings.

VI. CONCLUSIONS

In this paper we have shown that an ionic model is able to describe very satisfactorily the structure and the phonon dispersion relations of the cuprates. We find that it is possible to use the same empirical model parameters for the different cuprates with a few exceptions. In particular, the 123 system requires either the explicit use of a covalent potential [Cu(1)-O(4) in O_6] or to introduce special force constants [O(1)-O(4) in O_7] to achieve stability

of the crystal lattice. For the T and the T' compounds there is no absolute need to use special force constants although tuning of a single force constant significantly improves the fit to the structural data (La_2CuO_4) or to the dispersion relation (Nd_2CuO_4). These shortcomings suggest that a purely ionic model is not fully appropriate and that other terms, in particular three-body covalent interactions, should be included in the model. We would like to point out that some part of the three-body interactions is effectively included through the oxygen-oxygen interactions.

A decisive test of the proposed model will be its application to further members of the cuprate family. The model turned out to be quite successful to explain unexpected changes of the phonon intensities when going from the tetragonal to the orthorhombic phase of La_2CuO_4 . These results will be given elsewhere.³⁰ Extension of the model to Bi-2212 yielded a satisfactory repro-

duction of the PDOS. On the other hand, preliminary calculations for the new Hg-based superconductors indicate that the model is not fully adequate in this case. This can be traced to the relatively low packing density of the atomic structure in the compounds which makes the neglect of the covalent part of the binding forces more serious (as in the 123 compounds). Whereas in densely packed structures three-body forces can be mimicked easily by second-nearest-neighbor two-body forces, this is no longer true in relatively open structures. Nevertheless, we feel that the model presented in this paper will be a good starting point in all cases.

ACKNOWLEDGMENT

S.L.C. thanks the Alexander von Humboldt Foundation for financial support.

*Permanent address: Solid State Physics Division, Bhabha Atomic Research Centre, Bombay 400085, India.

†Present address: Institut Laue-Langevin, B.P. 156, F-38042 Grenoble Cedex 9, France.

¹L. Pintschovius, *Festkörperprobleme, Advances in Solid State Physics* Vol. 30, edited by V. Rössler (Vieweg, Braunschweig, 1990), p. 183; L. Pintschovius, N. Pyka, W. Reichardt, A. Yu. Rumiantsev, N. L. Mitrofanov, A. S. Ivanov, G. Collin, and P. Bourges, *Physica C* **185-189**, 156 (1991); W. Reichardt, F. Gompf, L. Pintschovius, N. Pyka, B. Renker, P. Bourges, G. Collin, A. S. Ivanov, N. C. Mitrofanov, and A. Yu. Rumiantsev, in *Electron-Phonon Interaction in Oxide Superconductors*, Proceedings of the First CINVESTAV Superconductor Symposium, edited by R. Baquero (World Scientific, Singapore, 1991), p. 1; L. Pintschovius, N. Pyka, W. Reichardt, A. Yu. Rumiantsev, N. L. Mitrofanov, A. S. Ivanov, G. Collin, and P. Bourges, *Physica B* **174**, 323 (1991); N. Pyka, W. Reichardt, L. Pintschovius, and G. Collin, in Proceedings of the IV International School on Neutron Physics, Alushta, edited by M. N. Saradudin (Dubna-Report, 1991), p. 314. In addition to the data reported in these publications some unpublished data of the authors have been used in the present work, too.

²R. E. Cohen, W. E. Pickett, and H. Krakauer, *Phys. Rev. Lett.* **62**, 831 (1989); **64**, 2575 (1990).

³O. K. Andersen, A. I. Liechtenstein, O. Rodriguez, I. I. Mazin, O. Sepson, V. P. Antropov, O. Gunnarson, and S. Gopalan, *Physica C* **185-189**, 147 (1991).

⁴W. Reichardt, L. Pintschovius, and N. Pyka (unpublished).

⁵(a) V. Prade, A. D. Kulkarni, F. W. de Wette, W. Kress, M. Cardona, R. Reiger, and V. Schröder, *Solid State Commun.* **64**, 1267 (1987); (b) R. Liu, C. Thomsen, W. Kress, M. Cardona, B. Gegenheimer, F. W. de Wette, J. Prade, A. D. Kulkarni, and V. Schröder, *Phys. Rev. B* **37**, 7971 (1988); (c) W. Kress, V. Schröder, J. Prade, A. D. Kulkarni, and F. W. de Wette, *ibid.* **38**, 2906 (1988); (d) A. D. Kulkarni, F. W. de Wette, J. Prade, V. Schröder, and W. Kress, *ibid.* **43**, 5451 (1991); (e) E. Rampf, V. Schröder, F. W. de Wette, A. D. Kulkarni, and W. Kress, *ibid.* **48** 10 143 (1993).

⁶(a) S. L. Chaplot, *Phys. Rev. B* **37**, 7435 (1988); (b) *Phase Trans.*

19, 49 (1989); (c) *Phys. Rev. B* **42**, 2149 (1990); (d) **45**, 4885 (1992); (e) (unpublished); (f) N. Choudhury, K. R. Rao, and S. L. Chaplot, *Physica C* **171**, 567 (1990).

⁷M. Mostoller, Jiquong Zhong, A. M. Rao, and P. C. Eklund, *Phys. Rev. B* **41**, 6488 (1990).

⁸See, e.g., P. Brüesch, *Phonons: Theory and Experiments I*, Springer Series in Solid State Sciences Vol. 34 (Springer, Berlin, 1982).

⁹G. D. Mahan, *Many-Particle Physics*, 2nd ed. (Plenum, New York, 1990), Chap. 5.

¹⁰M. Born and K. Huang, *Dynamical Theory of Crystal Lattices* (Clarendon, Oxford, 1954).

¹¹K. K. Yin *et al.*, *Austr. J. Phys.* **45**, 221 (1992).

¹²B. Renker, F. Gompf, P. Adelman, T. Wolf, H. Mutka, and A. Dianoux, *Physica B* **180&181**, 450 (1992).

¹³D. V. Fil, O. I. Tokov, A. C. Shelankov, and W. Weber, *Phys. Rev. B* **45**, 5633 (1992).

¹⁴W. Weber, *Phys. Rev. Lett.* **58**, 1371 (1987).

¹⁵D. J. W. Geldart and S. H. Vosko, *Can. J. Phys.* **44**, 2137 (1966).

¹⁶W. Reichardt, M. van Berg, and L. Weiss (unpublished).

¹⁷N. Pyka, N. L. Mitrofanov, P. Bourges, L. Pintschovius, W. Reichardt, A. Yu. Rumiantsev, and A. S. Ivanov, *Europhys. Lett.* **18**, 711 (1992).

¹⁸M. Braden, W. Paulus, A. Cousson, P. Vigoureux, G. Heger, A. Gukassov, P. Bourges, and D. Petigand, *Europhys. Lett.* **25**, 625 (1994).

¹⁹W. Reichardt, L. Pintschovius, N. Pyka, P. Schweiss, A. Erb, P. Bourges, G. Collin, J. Rossat-Mignod, L. P. Henry, A. S. Ivanov, N. L. Mitrofanov, and A. Yu. Rumiantsev, *J. Supercond.* **7**, 399 (1994).

²⁰E. T. Heyen, R. Liu, M. Cardona, S. Pinol, R. S. Melville, D. Mc K. Paul, E. Morán, and M. A. Alavio-Franco, *Phys. Rev. B* **45**, 2857 (1991).

²¹B. Renker, F. Gompf, E. Gering, D. Ewert, H. Rietschel, and A. Dianoux, *Z. Phys. B* **73**, 309 (1988).

²²C. Thomsen, R. Liu, M. Bauer, A. Wittlin, C. Genzel, M. Cardona, E. Schönherr, W. Bauhofer, and W. König, *Solid State Commun.* **65**, 55 (1988).

²³G. Burns, F. M. Dacol, C. Feild, and F. Holtzberg, *Solid State*

- Commun. 77, 367 (1991).
- ²⁴N. Pyka, W. Reichardt, L. Pintschovius, S. L. Chaplot, P. Schweiss, A. Erb, and G. Müller-Voigt, Phys. Rev. B **48**, 7747 (1993).
- ²⁵W. Reichardt, L. Pintschovius, N. Pyka, P. Schweiss, A. Erb, P. Bourges, G. Collin, J. Rossat-Mignod, I. Y. Henry, A. S. Ivanov, M. C. Mitrofanov, and A. Yu. Rumiantsev, J. Supercond. **7**, 399 (1994).
- ²⁶P. Schweiss, W. Reichardt, M. Braden, G. Collin, G. Heger, H. Claus, and A. Erb, Phys. Rev. B **49**, 1387 (1994).
- ²⁷M. Lei, J. L. Sarrao, W. M. Visscher, T. M. Bell, J. D. Thompson, A. Migliori, V. W. Welp, and B. W. Veal, Phys. Rev. B **47**, 6154 (1993).
- ²⁸N. F. Wright and W. H. Butler, Phys. Rev. B **42**, 4219 (1990).
- ²⁹H. Nozaki and S. Itoh, Phys. Rev. B **48**, 7583 (1993).
- ³⁰S. L. Chaplot, W. Reichardt, and L. Pintschovius (unpublished).